Virology Journal

RESEARCH

Open Access

Characterization of an unusual tobacco rattle virus isolate and a novel phenuivirid in the Jerusalem sage

Mathieu Mahillon[1,2], Nathalie Dubuis[1], Justine Brodard[1], Isabelle Kellenberger[1], Arnaud G. Blouin[1] and Olivier Schumpp[1*]

Abstract

Background The Jerusalem sage (*Phlomis fruticosa*) is a popular ornamental in Europe. In 2022, typical virus-like symptoms consisting of chlorotic rings and irregular patches were identified on leaves of this plant species in Lausanne, Switzerland.

Methods High-throughput sequencing was used on symptomatic samples, which was followed by transmission electron microscopy, sap inoculations of indicator species, and RT-PCR analyses.

Results Two RNA viruses were identified. The first one represents a novel isolate of tobacco rattle virus (TRV) named "Phlo". Its presence was confirmed in symptomatic plants but not in asymptomatic ones. Phlo is distinguished by its exceptionally long RNA2 that harbours a peculiar genetic make-up, which could be associated with host-specific systemic infection ability. The second virus, detected both in symptomatic and asymptomatic sages, is a novel member of the family *Phenuiviridae* named "phlomis phenuivirus 1" (PPV1). PPV1 exhibits a "cogu-like" architecture with a bi-segmented, ambisense RNA genome encoding a replicase, nucleocapsid, and putative movement protein. PPV1 is related to muscari virus A, and together they likely constitute a new genus for which the name "Maladivirus" is proposed.

Conclusions TRV Phlo is most likely responsible for the symptoms observed on the Jerusalem sages. PPV1 may be latent on this species, although there are still uncertainties regarding its host.

Keywords Bunyaviricetes, Coguvirus, Entovirus, Phenuiviridae, Phlomis, Tobravirus, TRV, Virgaviridae

*Correspondence:
Olivier Schumpp
olivier.schumpp@agroscope.admin.ch
[1]Research group Virology, Bacteriology and Phytoplasmology, Plant Protection Department, Agroscope, Switzerland
[2]Department of Plants and Crops, Faculty of Bioscience Engineering, Ghent University, Ghent, Belgium

Introduction

Advances in high-throughput sequencing (HTS) technologies have revolutionized plant virology. HTS allows for the unbiased analysis of nucleic acids, which is particularly relevant in the cases of untransmissible and/or latent phytoviruses that would be otherwise omitted by traditional diagnostic methods. HTS has therefore significantly expanded the known plant virome [1], and has become increasingly popular in routine phytosanitary analyses as costs decrease [2]. Here, we used HTS to investigate the etiology of diseased plants of the Jerusalem sage (*Phlomis fruticosa*), an ornamental in the family *Lamiaceae*. Native to the eastern Mediterranean regions, this evergreen shrub is widely grown across Europe for its attractive yellow flowers. This species can readily propagate over several years in temperate areas, which favors a potential role as pathogen reservoir. So far, the sole virus identified in Jerusalem sage is phlomis mottle virus (PhMV), a trichovirus discovered in Italy [3]. Our HTS analysis of symptomatic Jerusalem sages revealed the mixed infection of an atypical isolate of tobacco rattle virus (TRV, *Tobravirus tabaci*) and a novel virus belonging to the family *Phenuiviridae*.

TRV is a member of the genus *Tobravirus* (family *Virgaviridae*; order *Martellivirales*) which also accommodates pea early-browning virus (PEBV, *Tobravirus pisi*) and pepper ringspot virus (PRV, *Tobravirus capsica*) [4]. The history of TRV dates back to the late 1890s in Germany, when the "Mauche" disease was first reported on tobacco [5]. Nowadays, although TRV is best known as a versatile biotechnology tool [6], it still remains problematic on ornamentals and crops such as potato. TRV is ubiquitous in many agricultural soils worldwide, inducing latent to strongly symptomatic infections [7]. Its host range is exceptionally wide, encompassing over 400 plant species from 50 families [7]. The virus is transmitted by nematodes from the genera *Paratrichodorus* and *Trichodorus*, and actively attracts these vectors through modulation of plant root volatiles [8]. Transmission can also occur via seeds [9]. TRV genome consists of two positive sense, single-stranded RNAs (RNA1 and 2) encapsidated in rod-shaped virions [10]. Both RNAs are 5'-capped and have a 3'-tRNA structure [11]. RNA1 encodes the subunits of the RNA-dependant RNA polymerase (RdRp), a movement protein (MP) and a cysteine-rich protein (CRP). Both the MP and CRP act as viral suppressors of RNA silencing [12, 13], and a recent study has also highlighted a role in virion formation for the CRP [14].

While TRV RNA1 is highly stable among isolates [6], RNA2 is prone to reassortment, recombination, insertion and deletion [15]. Two main architectures have been described for this RNA. The most common architecture consists of the capsid protein (CP) ORF located in 5', which is followed by the ORFs encoding 2b and 2c, two proteins involved in nematode transmission [16]. Some isolates exhibiting this architecture have shortened versions of 2b and/or 2c, and a few isolates have additional small ORFs in the 3' region [17]. The second RNA2 architecture, previously framed as "rule-breaking" architecture, consists of the CP ORF preceded by one or several ORFs. It was first described for the "Spinach Yellow Mottle" (SYM) isolate in England in 1979, for which RNA2 harbours three CP-preceding ORFs encoding hypothetical proteins (HPs) [18, 19]. In 2014, the Polish isolate Mlo7 identified in potato was also predicted to encode a small CP-preceding HP closely related to one of SYM HPs [20]. A similar architecture was found in 2015 for the German isolates Da and Db, both retrieved from strongly-symptomatic potato tubers, and encoding a CP-preceding HP of 35 kDa (35 K) unrelated to SYM HPs [21]. Last, the RNA2 of the isolate IFA65, first identified in Italy on pepper in the 1970s [22], has been recently sequenced, revealing a long CP-preceding ORF related to SYM HPs [22]. The biological role of all these aforementioned CP-preceding ORFs remains unknown.

The family *Phenuiviridae* (order *Hareavirales*; class *Bunyaviricetes*) accommodates viruses with negative and ambisense RNA infecting eukaryotes, including humans [23–26]. These viruses have segmented genomes encoding at least an RdRp and a nucleocapsid (N). While many phenuivirids produce glycoproteins and are protected in an envelope, others are "naked" and appear as flexuous filaments consisting of genomic RNA associated with N proteins. This is the case for plant phenuivirids such as members of the genera *Tenuivirus*, *Mechlorovirus*, *Cogu-virus* and *Rubodvirus* [27–31]. In recent years, *Phenuiviridae* has greatly expanded through the accumulation of HTS data, which has led the International Committee on Taxonomy of Viruses to recognize several new "cogu-like" genera: *Entovirus*, *Laulavirus*, *Lentinuvirus* and *Bocivirus*. These viruses are presumably naked and encode an RdRp, N, and putative MP that is structurally similar to proteins from the tobacco mosaic virus 30 kDa family [32, 33]. Cogu-like viruses have been retrieved from various eukaryotes (plants, fungi, arthropods) and environmental samples [34–39]. Remarkably, a recent study has shown that the laulavirus valsa mali negative-strand RNA virus 1 (VmNSRV1) can be found in natural populations of fungi and plants, leading to its description as the first "phyto-mycovirus" [40].

Material and method

Plant material and sap inoculations

Leaves of asymptomatic and symptomatic plants of Jerusalem sage were collected in a private garden in Lausanne (Switzerland), in proximity to the so-called "Maladière" area in August 2022. Symptomatic leaves were used for

the mechanical inoculation of several indicator plant species. Briefly, a sap inoculum was produced by grinding leaves in cold phosphate buffer (1 mM sodium diethyldithiocarbamate, 20 mM Na_2HPO_4, pH 7.6) in a mortar using a pestle. The resulting sap was rubbed on the first true leaves of indicator species using carborundum (400-mesh silicon carbide, Aldrich) as abrasive. Tested plants included sugar beet (*Beta vulgaris*), *Chenopodium (C. quinoa* and *C. amaranticolor*), tobacco (*Nicotiana tabacum* and *N. benthamiana*) and periwinkle (*Catharanthus roseus*). After inoculation, plants were maintained in greenhouses (24 °C, 14/10 h photoperiod) for one month with daily inspections.

Virion observation and inoculation

For the visualisation of virions, a simplified protocol dedicated to the semi-purification of TRV particles was followed [41]. Briefly, 10 g of symptomatic sage leaves were first ground in liquid nitrogen in a mortar using a pestle. The resulting powder was mixed with 20 ml of CP buffer (0.18 M McIlvaine buffer, pH 7) supplemented with 0.2% thioglycolic acid, and squeezed through a nylon filter cloth. One volume of 1:1 diethylether: carbon tetrachloride was added, followed by slow mixing for 5 min. The phases were then separated by low-speed centrifugation (20 min, 4,000 rpm) and the upper phase was used for high-speed centrifugation (1 h, 40,000 rpm). The resulting pellet was suspended in 1 mL CP buffer. The low and high-speed centrifugation steps were repeated, and the final pellet was resuspended in 0.1 mL CP buffer. Particles were observed by transmission electron microscopy (TEM) using the Tecnai G2 Spirit electron microscope as previously described [42]. Semi-purified particles were also used for plant inoculation as described in the previous section.

RNA extraction, RT-PCR and HTS

Total RNA was extracted from symptomatic or asymptomatic leaves using a 3% CTAB protocol, which was followed by DNase treatment as previously described [43]. RNA concentration was estimated with the Qubit 3 Fluorometer (Invitrogen). RT-PCR analyses were conducted on these samples using the M-MLV reverse transcriptase and the Go Taq polymerase (Promega) as described before [43]. The primer pair Katu/Katd was used to assess the presence of PhMV [44]. TRV RNA1 was amplified using the primer pair TRV_F/R [45], while the new primer pair TRV2JS_F/R (TCGGGGTTTACTTGGTTCCG/CTCCTAACGCATTGTTGGCG) was designed to amplify RNA2. The segments L and S of the phenuivirid were amplified using the pairs PPV1_F2/R2 (GCTAGGGACGATGCAGAGGG/GCACCTGAGCTTTGTAGACGC) and PPV2_F1/R1 (CCGCCAGAGTGAGTGAGAGG/AGACAGAGCAAGGAGGCGAG). All primer pairs were used for PCR with an annealing temperature of 65 °C. PCR amplicons were analysed by agarose gel electrophoresis.

The DNase-treated RNA extracted from 0.5 g of leaves from two plants was sent to Macrogen (South Korea) for an Illumina sequencing as previously documented [46]. A total of 95,985,190 reads were generated, of which 93.6% exhibited high quality scores (> Q30) and were further used for trimming using Trimmomatic [47] and *de novo* assembly with Spades [48]. Contigs longer than 500 bp were then submitted to BlastX searches against a local virus database. Contigs with hits E-value < 0.001 were further examined by online BlastX and BlastN searches.

Bioinformatics analyses

Viral genomes were analysed using Jalview [49] and UGENE [50]. Functional annotation was performed using the MOTIF web server (https://www.genome.jp/tools/motif/). Accession numbers for the proteins used in this study are available in Table S1 (for tobraviruses) and S2 (for phenuivirids). Protein alignments were obtained using Muscle [51]. For phylogenetic analyses, alignments were first loaded into ModelFinder [52] in order to find the best aa substitution model. Maximum-likelihood (ML) phylogenetic trees were then built with IQ-Tree [53] in combination with ultrafast bootstrap [54]. The ML trees were manually curated on ITol [55]. RNA secondary structures were predicted using the RNAfold web server [56]. Homologs of viral proteins in fungal genomes were further screened on the MycoCosm portal [57].

Results

A new TRV isolate

In the summer 2022, large chlorotic rings and irregular patches were noted on leaves of Jerusalem sages in a private garden in Lausanne (Fig. 1A). Total RNA extracted from one symptomatic leaf tested negative for PhMV by RT-PCR, suggesting the presence of another causal agent. Sap inoculations of several indicator species were unsuccessful, and examination of crude extracts by TEM did not reveal viral particles. Furthermore, a cellulose-based extraction protocol failed to evidence any dsRNA element in the leaves (data not shown). Altogether, these results prompted an HTS analysis of total RNA. Following *de novo* assembly and Blast analyses, two viral contigs (6,752 and 4,590 nt) were identified, corresponding to the RNA1 and 2 of a new TRV isolate. Both contigs were assembled with high coverages (1,547x and 691x, respectively) and exhibited partial TRV termini (data not shown), indicating near-complete sequencing. This new TRV isolate is hereafter dubbed "Phlo", and its RNA1 and RNA2 sequences are available in NCBI Genbank under accession numbers PV297904 and PV297905, respectively.

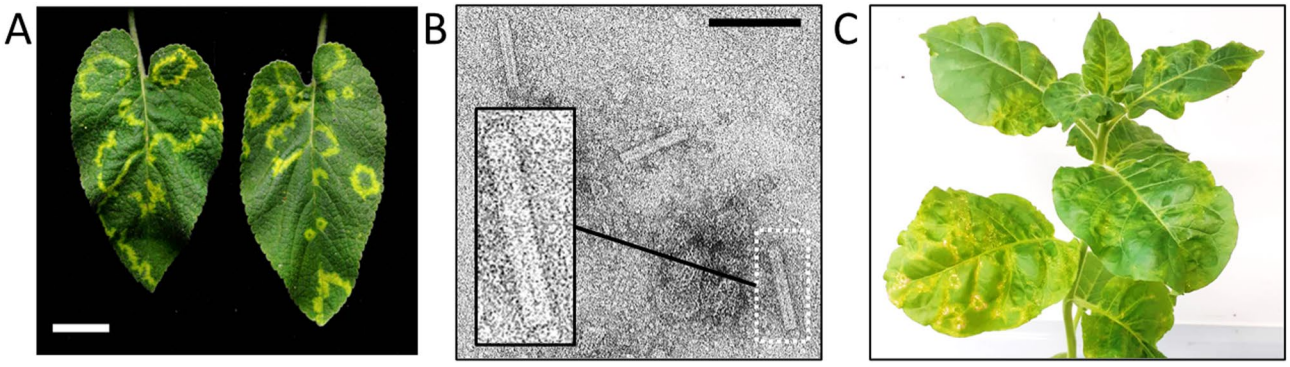

Fig. 1 Symptoms and particles associated with TRV Phlo. (**A**) Leaves of Jerusalem sages with virus-like symptoms that were used for the HTS analysis. The white bar represents 1 cm. (**B**) Electron micrograph of three TRV Phlo virions. Particles were stained with phosphotungstic acid. The black bar represents 100 nm. The inner panel gives a closer look at the central canal. (**C**) Mosaic and ringspot symptoms on upper leaves of *N. tabacum* cv. Xanthii, 30 days post inoculation with semi-purified TRV Phlo particles

RT-PCR analyses confirmed the presence of Phlo RNA1 and 2 in four symptomatic leaves of Jerusalem sages, while there was no detection in four samples from asymptomatic sages collected at the same location (Fig. S1). Rod-shaped particles (ca. 50–150 nm in length) were observed in semi-purified extracts from sage leaves (Fig. 1B). These particles exhibited a clear central canal, in line with previous characterization of TRV virions [10]. Mechanical inoculation using semi-purified virions was successful on several indicator plants. Mild chlorosis appeared at 4 days post inoculation (dpi) on leaves of both *N. benthamiana* and *N. tabacum*, but systemic symptoms were only noted on the latter. On this species, ringspots and severe mosaic developed locally at 7 dpi, and later spread on upper tissues as well (Fig. 1C). Periwinkles did not exhibit local symptoms but showed chlorotic spots on upper leaves after one week. Conversely, plants of sugar beet developed local chlorotic spots at 7 dpi, but no systemic symptom was noted. Chlorotic and necrotic spots appeared 3 dpi on the inoculated leaves of the two *Chenopodium* species. Inoculated leaves of *C. quinoa* eventually became completely necrotic and collapsed. After one week, chlorosis, vein necrosis and deformations were noted on the upper leaves of these species (Fig. S2). This last result is quite remarkable as long-distance movement in *Chenopodium* has only been reported for SYM among TRV isolates [18].

Analysis of phlo genome

Phlo RNA1 is highly similar to other TRV RNA1s, showing a classic architecture, with the closest sequence being ppk20 RNA1 (AF406990.1, 100% cover, 99.5% nt id.). In contrast, Phlo RNA2 is rather unusual, as it is longer than other reported TRV RNA2 and harbours five long (> 200 nt) ORFs dubbed "ORF1-5" (Fig. 2A). BlastP searches on these ORFs yielded intriguing results (Table 1). Both ORF1 and 2 show homology to the CP-preceding HP of IFA65, but also to the HPs of SYM and Mlo7. ORF3 corresponds to the CP, while ORF4 encodes a distant homolog of 2b from TRV 11r21, an isolate collected at the same location of Mlo7 [20]. ORF5 hypothetically encodes a small protein of 9 kDa (9 K) that is also present on IFA65 RNA2, but does not show homology to any other sequence in the NCBI databases. Consistent with these results, a BlastN search on Phlo RNA2 yielded IFA65 RNA2 as the closest sequence (ON156783.1, 77% cover, 98% nt id.). Both RNAs are almost identical except for the 2b-encoding region lacking in IFA65 (Fig. 2A).

A phylogeny of the *Tobravirus* CPs, which is the only conserved gene in RNA2, reveals that most isolates fall in four main lineages: "alpha", "beta", "gamma", and "delta" (Fig. 2B), consistent with a previous study [21]. The isolates with CP-preceding ORFs belong to two groups within the alpha lineage, with Da and Db forming the "alpha 1" subclade, while Phlo and the remaining isolates are grouped into the "alpha 2" subclade (Fig. 2C). A third group, the subclade "alpha 3" accommodates isolates with a classic architecture shared with other TRV RNA2s. Hypothetically, three gene acquisitions occurred among members of the alpha 1 and 2 subclades, and several deletion events also occurred. 2b is truncated in SYM and totally lost in Mlo7 and IFA65. The CP-preceding HPs also have experienced deletions, with total lost in 11r21. An alignment of these HPs shows that no isolate seem to possess a full-length ancestral version (Fig. S3).

A novel phenuivirid

In addition to Phlo, a second RNA virus was identified in the HTS dataset. Indeed, two contigs (5,832 and 3,372 nt) were found harbouring ORFs related to proteins from phenuivirids (BlastX hits with E-value = 0). These contigs were thus assigned to the long (L) and short (S) segments of a novel virus tentatively named "phlomis phenuivirus 1" (PPV1, accession numbers PV370485 and PV370486). The sequencing coverages of PPV1 segments (71x and 141x, respectively) were significantly lower than that

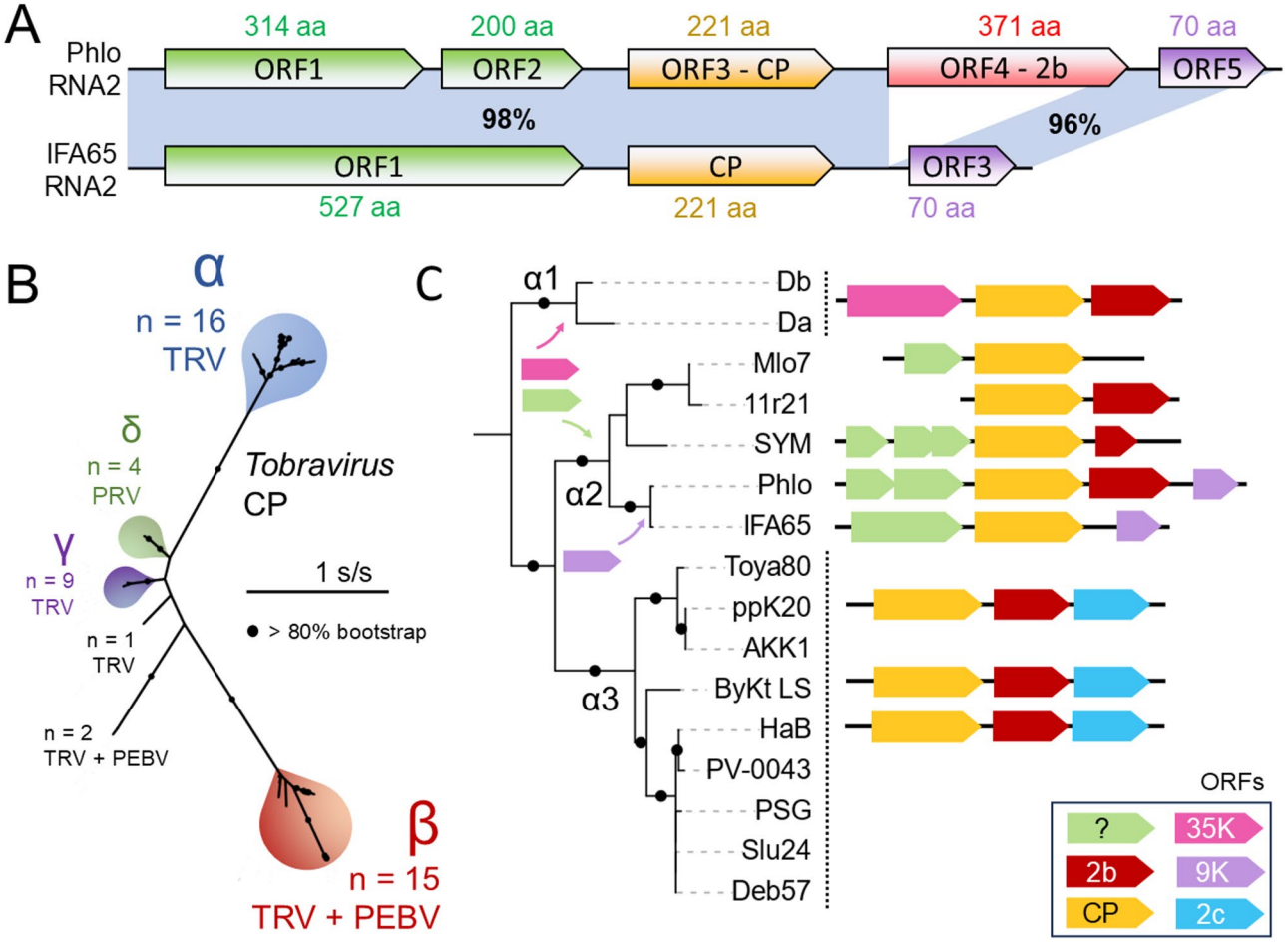

Fig. 2 Genomic and phylogenetic analyses of TRV Phlo RNA2. (**A**) Schematic representation of the RNA2s of Phlo and IFA65. Colored arrows represent ORFs. The shaded areas indicate nt identities (in percent). (**B**) Unrooted ML phylogenetic tree of the *Tobravirus* CPs (see Table S1 for accession numbers). The tree was built using the model JTT + G4. Black circles on branch indicate > 80% bootstrap support. "n" indicates the number of isolates in each clade. (**C**) Details on the alpha lineage within the CP tree. For each isolate, the corresponding RNA2 architecture is represented when available. Description of the ORFs are given in the lower right panel

Table 1 Description of the best blastp hits for the ORFs of TRV Phlo RNA2

ORF	Size (aa)	Best hit	Cover (%)	ID (%)	Size (aa)	Acc. number
1	314	IFA65 RNA2 ORF1	100	98	527	WCJ12589.1
2	200	IFA65 RNA2 ORF1	100	97	527	WCJ12589.1
3	221	IFA65 RNA2 CP	100	99	221	WCJ12590.1
4	371	11r21 RNA2 2b	99	47	369	AHG52767.1
5	70	IFA65 RNA2 ORF3	100	99	70	WCJ12591.1

of Phlo, indicating a lower viral titre. Interestingly, RT-PCR analyses showed the presence of PPV1 not only in symptomatic but also in asymptomatic leaves of Jerusalem sages (Fig. S1), suggesting that the virus might be latent on this species. A RACE protocol was followed to obtain the sequences of the RNA termini of PPV1, without success.

A representation of the genome of PPV1 is provided on Fig. 3A. PPV1 segment L encodes a large (partial) protein of 1,919 aa with the *Bunyavirus* RdRp domain pfam04196 at positions 615–1286. PPV1 segment S is ambisense, harbouring two ORFs in opposite frames. The 425 nt-long intergenic region separating these ORFs is highly rich in AT, and it is predicted to fold into a stable secondary structure (Fig. 3B), which are features described in many phenuivirids. The first ORF of PPV1 segment S encodes a protein of 359 aa containing the *Tenuivirus/Phlebovirus* N domain pfam05733 (positions 47–307), and the second ORF encodes a HP of 448 aa with no known domain. Nevertheless, BlastP search on this HP revealed distant homology (< 30% aa id.) with the putative MPs associated with several other cogu-like viruses.

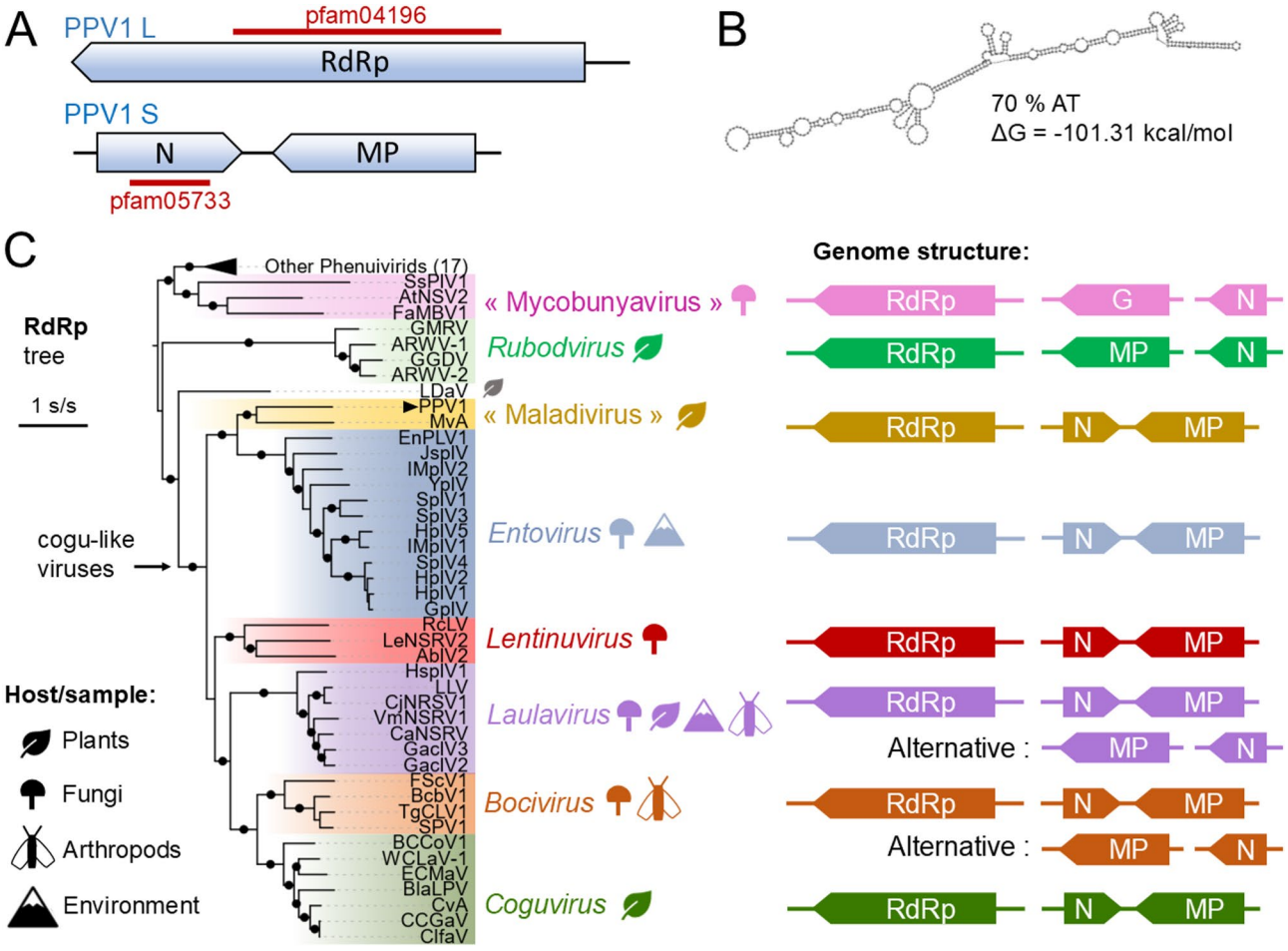

Fig. 3 Genomic and phylogenetic analyses of PPV1. (**A**) Schematic representation of PPV1 genomic segments L and S. Colored arrows represent ORFs. (**B**) Predicted secondary structure for PPV1 segment S intergenic region. The percentage of AT and minimal energy are indicated. (**C**) Left: ML phylogenetic tree for the RdRp of PPV1 and related phenuiviridids. The tree was built using the substitution model rtREV + I + G4. Black circles on branch indicate > 80% bootstrap support. The position of PPV1 is indicated by a black arrow. Right: Genome architectures. RdRp: RNA-dependant RNA polymerase; G: glycoprotein; N: nucleocapsid; MP: movement protein

Phylogenetic analyses of PPV1

ML phylogenetic trees were built for PPV1 proteins and their homologs from representative phenuiviridids (Table S2). In the RdRp tree (Fig. 3C, left panel), PPV1 is placed in a strongly-supported clade with muscari virus A (MvA), a virus identified by HTS in grape hyacinth (*Muscari neglectum*) in Western Australia [58]. Both viruses arguably form a new genus of cogu-like viruses as their RdRp share very low level of aa identities (< 37%) with the closest sequences. We propose therefore the novel genus "Maladivirus" (from the location of the sampled sages in the "*Maladi*ère" area) to accommodate PPV1 and MvA.

Maladiviruses represent a sister clade of the genus *Entovirus* that consists of the mycovirus entoleuca phenui-like virus 1 (EnPLV1) and sequences retrieved from metaviromics studies of soils and sediments in China [59, 60]. The genera "Maladivirus" and *Entovirus* share a common bi-segmented genome architecture with other cogu-like viruses, with some exceptions found among laulaviruses and bociviruses for which the N and MP ORFs are located on distinct segments (Fig. 3C, right panel).

In the phylogenetic tree of N proteins (Fig. 4A), which is not available for MvA, PPV1 appears again most closely related to entoviruses. In contrast to the RdRp and N that are shared with other phenuiviridids, the MPs of cogu-like are unique in the family *Phenuiviridae* and show distant homology to the MPs of ophioviruses (family *Aspiviridae*), which are negative-strand RNA viruses infecting a great diversity of plants [28, 32]. The MP tree was therefore built using ophioviruses' MPs as outgroup (Fig. 4B). In this tree, cogu-like viruses form two distinct clades, with maladiviruses again closely related to several members of the genus *Entoviruses*. The MPs of maladiviruses and entoviruses appear also related to the MPs of lentinuviruses, which have been exclusively associated with fungi [36, 61]. Interestingly, in both N and MP trees, a few phylogenetic incongruences appear among

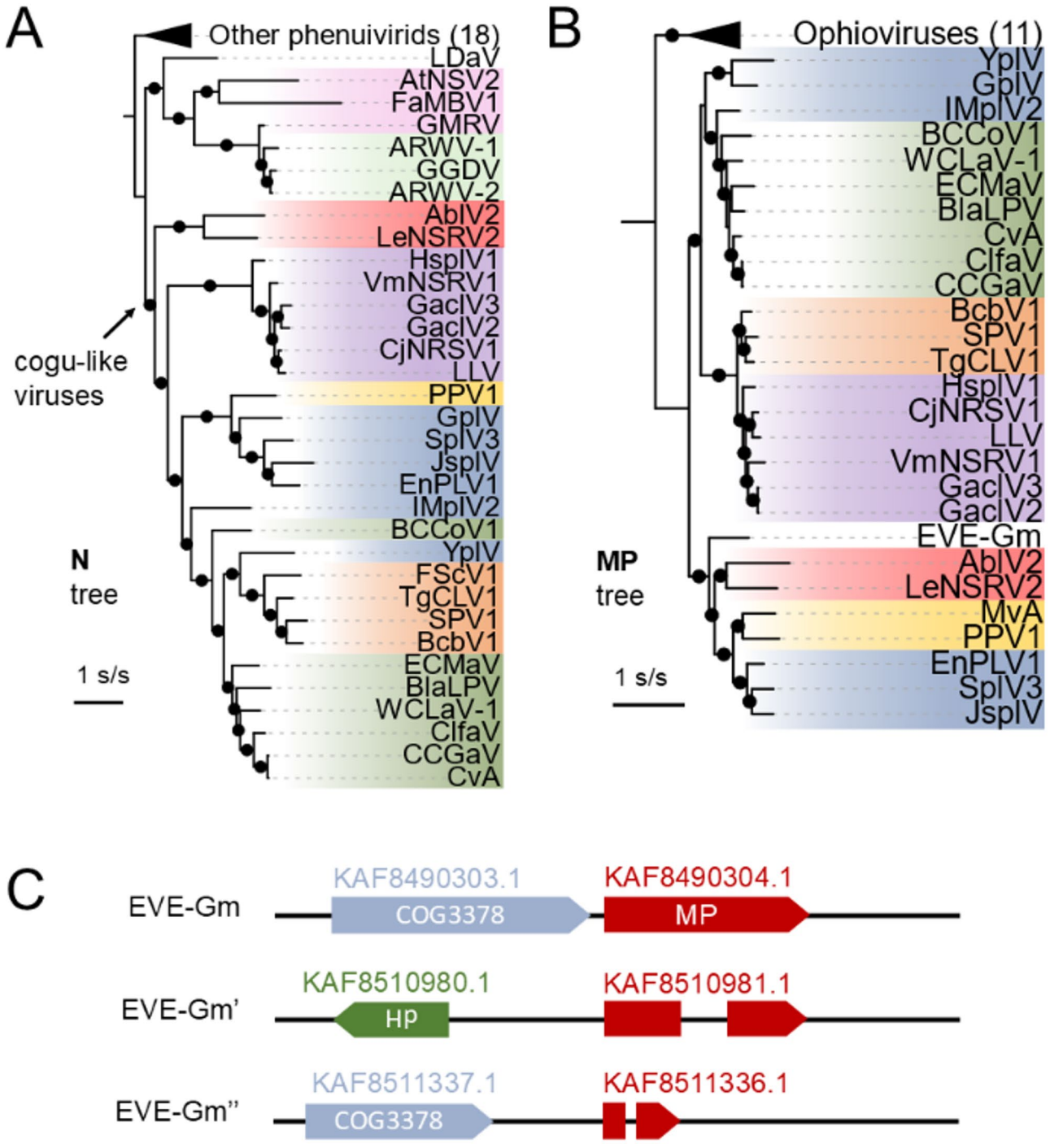

Fig. 4 ML phylogenetic trees for the proteins N (**A**) and MP (**B**) of PPV1 and related phenuivirids. The trees were built using the substitution models LG + F + G4 and rtREV + F + I + G4, respectively. Black circles on branch indicate > 50% bootstrap support. Colored boxes represent genera as indicated on Fig. 3C. **C.** Schematic representation of the three endogenous viral elements detected in the genome of *G. morchelliformis* GMNE.BST

coguviruses and entoviruses, suggesting possible events of recombination/reassortment.

Curiously, an online BlastP search revealed a distant homolog of PPV1 MP (KAF8490304.1, 366 aa, 64% cover, 27% id.) in the genome of the mycorrhizal fungus *Gautieria morchelliformis* strain GMNE.BST (assembly "Gaumor1_1", acc. number: GCA_015179125.1 [62]). The associated ORF likely represents an endogenous viral element (dubbed EVE-Gm) which presumably results from the reverse-transcription and integration of a viral sequence into its host genome [63]. A previous study already evidenced an EVE related to lentinuviral N in

Table 2 Endogenous viral elements homolog to PPV1 MP in *G. morchelliformis* GMNE.BST

EVE	Scaffold	CDS positions	Strand	CDS accessions	Size (aa)
Gm	401	67,301 – 68,401	+	KAF8490304.1	366
Gm'	158	206,30 1-206,667 and 206,884 – 207,395	+	KAF8510981.1	292
Gm''	153	207,359 – 207,644 and 207,720 – 207,760	-	KAF8511336.1	108

the genome of the powdery mildew pathogen *Erysiphe cichoracearum* [36]. EVE-Gm is specifically related to the MPs of maladiviruses, entoviruses and lentinuviruses (Fig. 4B). Additional BlastN searches revealed two other similar EVEs (EVE-Gm' and EVE-Gm'', Table 2) on other scaffolds of the same assembly. These sequences are truncated and likely correspond to pseudogenized EVEs. In terms of genomic neighbourhood, EVE-Gm and EVE-Gm'' are preceded by an ORF harbouring the domain COG3378 (Fig. 4C), corresponding to a DNA primase/helicase associated with mobile genetic elements (MGE). BlastP search on this ORF yielded significant hits in other fungal genomes (data not shown), suggesting that it may represent a fungus-specific MGE. In the case of EVE-Gm', the MP-related ORF is followed by a HP with no known domain.

Discussion

Our HTS analysis revealed the mixed infection of two RNA viruses in symptomatic samples of Jerusalem sages. Genome analysis for these viruses provides interesting evolutionary insights for two distant taxa within the *Riboviria* realm.

A near-complete genome was reconstructed for Phlo, which corresponds to a new TRV isolate most likely responsible for the chlorotic patches and ring patterns observed on the sages. These symptoms are indeed consistent with those previously described on other plant species upon TRV infection [7]. Of particular interest, Phlo RNA2 is remarkably long, and is closely related to the RNA2s of the European isolates IFA65, SYM, Mlo7, and 11r21. All these RNA2s presumably derive from a common ancestor that acquired one (or multiple) CP-preceding ORF, and experienced various deletion events. Similar deletions have been previously reported for other TRV RNA2s upon repeated mechanical inoculations or extended *in planta* infection [21, 64]. As for the CP-preceding HPs, their function remain uncertain. Reverse genetics studies on SYM mutants lacking HPs have not revealed changes in viral titre or spread in *N. benthamiana* [19]. Nevertheless, early studies on this isolate have linked its RNA2 with long-distance movement in *C. quinoa*, an ability that is shared by Phlo but absent in isolates with a common architecture [18, 65]. Hence, the CP-preceding HPs might be involved in systemic infection in a host-specific manner. This could be easily experimentally tested using infectious clones in future research. It is important to highlight that most TRV sequences available to date have been obtained from potato. Consequently, further characterization of isolates from alternative hosts is warranted to improve our understanding of the genomic diversity of this virus.

The second RNA virus identified in the sages is the novel phenuivirid PPV1. This virus is likely latent on sages, although it is possible that it exacerbated the symptoms induced by TRV Phlo. Together with MvA, PPV1 belongs to the proposed genus "Maladivirus" within the large group of cogu-like viruses. A fascinating aspect of these viruses lies in their host diversity. Some cogu-like genera appear to be associated with one host kingdom as seen for coguviruses that infect plants and lentinuviruses that infect fungi. This could also be the case for *Bocivirus*, for which all members have been described as mycoviruses, except sanya phenuivirus 1 detected in a horse fly. The host range of *Laulavirus* seems wider, as suggested by the capacity of VmNSRV1 to infect both plants and fungi, and the identification of other laulaviruses in plants, fungi and arthropods. The case of *Entovirus* is unclear as the host status has only been clearly established for the mycovirus EnPLV1, whereas other members of this genus have been obtained from metaviromics studies of soils and sediments. As far as maladiviruses are concerned, both MvA and PPV1 might represent phytoviruses. However, clear demonstration of plant infection is still needed, as it is possible that these viruses actually infect plant-associated organisms (e.g. fungal endophytes) rather than plants themselves. Altogether, the host diversity of cogu-like viruses remind the case of members the family *Partitiviridae*, which are dsRNA viruses detected in multiple eukaryotic kingdoms. A recent study has demonstrated replication of several partitivirids in plants, fungi and animals [66], and this triple cross-kingdom infection capacity is worth testing for cogu-like viruses.

Another intriguing aspect of cogu-like viruses concerns their putative MPs. These proteins are arguably involved in the intercellular movement of coguviruses and plant-infecting cogu-like viruses, which is supported by the localization of VmNSRV1 MP in plasmodesmata [40]. However, the presence of such homologs in cogu-like viruses not associated with plants is puzzling. Either these proteins might be required during a hypothetical plant stage, or they could serve another function in non-plant hosts. Interestingly, the MPs of maladiviruses are particularly close to homologs found in mycoviruses as well as putative EVEs from the fungus *G. morchelliformis*.

These findings further question the true host of PPV1 and suggest a function in fungal hosts for these putative MPs.

Supplementary Information

The online version contains supplementary material available at https://doi.org/10.1186/s12985-025-02896-3.

Supplementary Material 1

Acknowledgements
We would like to thank Sabine Bonnard, Stefan Kellenberger, Marc Passerat and Larissa Grosu for taking care of the plants. We are also thankful to Jacques Mahillon and Raphaël Groux for critical review of the manuscript.

Author contributions
MM performed the plant sampling. ND and MM performed virus Purification and TEM. JB, IK and MM produced the HTS and conducted subsequent bioinformatics and molecular analyses. JB and MM performed biological assays. MM wrote the initial draft. AGB and OS critically reviewed the manuscript. All authors have read the manuscript and agree for publication.

Funding
This research received no external funding.

Data availability
No datasets were generated or analysed during the current study.

Declarations

Ethics approval and consent to participate
Not applicable.

Consent for publication
Not applicable.

Competing interests
The authors declare no competing interests.

Received: 2 May 2025 / Accepted: 24 July 2025
Published online: 06 August 2025

References

1. Dolja VV, Krupovic M, Koonin EV. Deep roots and splendid boughs of the global plant Virome. Annu Rev Phytopathol. 2020;58:23–53.
2. Lebas B, Adams I, Al Rwahnih M, Baeyen S, Bilodeau GJ, Blouin AG, et al. Facilitating the adoption of high-throughput sequencing technologies as a plant pest diagnostic test in laboratories: A step-by-step description. EPPO Bull. 2022;52(2):394–418.
3. Saldarelli P, Boscia D, De Stradis A, Vovlas C. A new member of the family flexiviridae from phlomis fructicosa. J Plant Pathol. 2008;90(2):281–6.
4. Adams MJ, Adkins S, Bragard C, Gilmer D, Li D, MacFarlane SA, et al. ICTV Virus Taxonomy Profile: Virgaviridae J Gen Virol. 2017;98(8):1999–2000.
5. Harrison BD, Robinson DJ. Tobraviruses. In: Van Regenmortel MHV, Fraenkel-Conrat H, editors. The plant viruses: the Rod-Shaped plant viruses. Boston, MA: Springer US; 1986. pp. 339–69.
6. Macfarlane SA. Tobraviruses–plant pathogens and tools for biotechnology. Mol Plant Pathol. 2010;11(4):577–83.
7. Adams MJ, Antoniw JF. DPVweb: a comprehensive database of plant and fungal virus genes and genomes. Nucleic Acids Res. 2006;34:D382–385.
8. van Griethuysen PA, Redeker KR, MacFarlane SA, Neilson R, Hartley SE. Virus-induced changes in root volatiles attract soil nematode vectors to infected plants. New Phytol. 2024;241(5):2275–86.
9. Cooper JI, Harrison BD. The role of weed hosts and the distribution and activity of vector nematodes in the ecology of tobacco rattle virus. Ann Appl Biol. 1973;73(1):53–66.
10. Nixon HL, Harrison BD. Electron microscopic evidence on the structure of the particles of tobacco rattle Virus582. Microbiology. 1959;21(3):582–90.
11. van Belkum A, Cornelissen B, Linthorst H, Bol J, Pley C, Bosch L. tRNA-like properties of tobacco rattle virus RNA. Nucleic Acids Res. 1987;15(7):2837–50.
12. Martín-Hernández AM, Baulcombe DC. Tobacco rattle virus 16-Kilodalton protein encodes a suppressor of RNA Silencing that allows transient viral entry in meristems. J Virol. 2008;82(8):4064–71.
13. Deng X, Kelloniemi J, Haikonen T, Vuorinen AL, Elomaa P, Teeri TH, et al. Modification of tobacco rattle virus RNA1 to serve as a VIGS vector reveals that the 29K movement protein is an RNA Silencing suppressor of the virus. Mol Plant Microbe Interact. 2013;26(5):503–14.
14. Yue N, Jiang Z, Pi Q, Yang M, Gao Z, Wang X, et al. Zn2+-dependent association of cysteine-rich protein with virion orchestrates morphogenesis of rod-shaped viruses. PLoS Pathog. 2024;20(6):e1012311.
15. Koenig R, Lesemann DE, Pleij CWA. Tobacco rattle virus genome alterations in the hosta hybrid 'green fountain' and other plants: reassortments, recombinations and deletions. Arch Virol. 2012;157(10):2005–8.
16. Macfarlane SA. Molecular determinants of the transmission of plant viruses by nematodes. Mol Plant Pathol. 2003;4(3):211–5.
17. Heinze C, Von Bargen S, Sadowska-Rybak M, Willingmann P, Adam G. Sequences of tobacco rattle viruses from potato. J Phytopathol. 2000;148(9–10):547–54.
18. Kurppa A, Jones AT, Harrison BD, Bailiss KW. Properties of spinach yellow mottle, a distinctive strain of tobacco rattle virus. Ann Appl Biol. 1981;98(2):243–54.
19. Ashfaq M, McGavin W, Macfarlane SA. RNA2 of TRV SYM breaks the rules for tobravirus genome structure. Virus Res. 2011;160(1–2):435–8.
20. Yin Z, Pawełkowicz M, Michalak K, Chrzanowska M, Zimnoch-Guzowska E. The genomic RNA1 and RNA2 sequences of the tobacco rattle virus isolates found in Polish potato fields. Virus Res. 2014;185:110–3.
21. Lindner K, Hilbrich I, Koenig R. Molecular characterization of variants of a new 'rule-breaking' tobacco rattle virus RNA2 in potatoes. Virus Res. 2018;244:270–5.
22. Conti M, Masenga V. Identification and prevalence of pepper viruses in Northwest Italy. J Phytopathol. 1977;90(3):212–22.
23. Herath V, Romay G, Urrutia CD, Verchot J. Family level phylogenies reveal relationships of plant viruses within the order bunyavirales. Viruses. 2020;12(9):1010.
24. Sun MH, Ji YF, Li GH, Shao JW, Chen RX, Gong HY, et al. Highly adaptive phenuiviridae with biomedical importance in multiple fields. J Med Virol. 2022;94(6):2388–401.
25. Sasaya T, Palacios G, Briese T, Di Serio F, Groschup MH, Neriya Y, et al. ICTV virus taxonomy profile: phenuiviridae 2023. J Gen Virol. 2023;104(9):001893.
26. Kuhn JH, Brown K, Adkins S, de la Torre JC, Digiaro M, Ergünay K, et al. Promotion of order bunyavirales to class bunyaviricetes to accommodate a rapidly increasing number of related Polyploviricotine viruses. J Virol. 2024;98(10):e01069–24.
27. Falk BW, Tsai JH. Biology and molecular biology of viruses in the genus tenuivirus. Annu Rev Phytopathol. 1998;36:139–63.
28. Navarro B, Zicca S, Minutolo M, Saponari M, Alioto D, Di Serio FA, Negative-Stranded RNA. Virus infecting citrus trees: the second member of a new genus within the order bunyavirales. Front Microbiol. 2018;9.
29. Lecoq H, Wipf-Scheibel C, Verdin E, Desbiez C. Characterization of the first tenuivirus naturally infecting dicotyledonous plants. Arch Virol. 2019;164(1):297–301.
30. Diaz-Lara A, Navarro B, Di Serio F, Stevens K, Hwang MS, Kohl J, et al. Two novel Negative-Sense RNA viruses infecting grapevine are members of a newly proposed genus within the family phenuiviridae. Viruses. 2019;11(8):685.
31. Gaafar YZA, Richert-Pöggeler KR, Sieg-Müller A, Lüddecke P, Herz K, Hartrick J, et al. A divergent strain of melon chlorotic spot virus isolated from black medic (Medicago lupulina) in Austria. Virol J. 2019;16(1):89.
32. Navarro B, Minutolo M, De Stradis A, Palmisano F, Alioto D, Di Serio F. The first phlebo-like virus infecting plants: a case study on the adaptation of negative-stranded RNA viruses to new hosts. Mol Plant Pathol. 2018;19(5):1075–89.
33. Butkovic A, Dolja VV, Koonin EV, Krupovic M. Plant virus movement proteins originated from jelly-roll capsid proteins. PLoS Biol. 2023;21(6):e3002157.
34. Chen YM, Sadiq S, Tian JH, Chen X, Lin XD, Shen JJ, et al. RNA Viromes from terrestrial sites across China expand environmental viral diversity. Nat Microbiol. 2022;7(8):1312–23.

35. Tokarz R, Sameroff S, Tagliafierro T, Jain K, Williams SH, Cucura DM, et al. Identification of novel viruses in amblyomma americanum, dermacentor variabilis, and Ixodes scapularis ticks. mSphere. 2018;3(2):e00614–17.
36. Lin YH, Fujita M, Chiba S, Hyodo K, Andika IB, Suzuki N, et al. Two novel fungal negative-strand RNA viruses related to mymonaviruses and phenuiviruses in the Shiitake mushroom (Lentinula edodes). Virology. 2019;533:125–36.
37. Bertazzon N, Chitarra W, Angelini E, Nerva L. Two new putative plant viruses from wood metagenomics analysis of an Esca diseased vineyard. Plants. 2020;9(7):835.
38. Kuhn JH, Adkins S, Alioto D, Alkhovsky SV, Amarasinghe GK, Anthony SJ, et al. 2020 taxonomic update for phylum Negarnaviricota (Riboviria: Orthornavirae), including the large orders Bunyavirales and Mononegavirales. Arch Virol. 2020;165(12):3023–72.
39. Sadiq S, Harvey E, Mifsud JCO, Minasny B, McBratney AB, Pozza LE, et al. Australian terrestrial environments harbour extensive RNA virus diversity. Virology. 2024;593:110007.
40. Dai R, Yang S, Pang T, Tian M, Wang H, Zhang D et al. Identification of a negative-strand RNA virus with natural plant and fungal hosts. Proceedings of the National Academy of Sciences. 2024;121(12):e2319582121.
41. Gugerli P. Different States of aggregation of tobacco rattle virus coat protein. J Gen Virol. 1976;33(2):297–307.
42. Mahillon M, Brodard J, Kellenberger I, Blouin AG, Schumpp O. A novel weevil-transmitted tymovirus found in mixed infection on Hollyhock. Virol J. 2023;20(1):17.
43. Mahillon M, Groux R, Bussereau F, Brodard J, Debonneville C, Demal S, et al. Virus yellows and syndrome basses richesses in Western switzerland: A dramatic 2020 season calls for urgent control measures. Pathogens. 2022;11(8):885.
44. Dovas CI, Katis NI. A spot nested RT-PCR method for the simultaneous detection of members of the vitivirus and foveavirus genera in grapevine. J Virol Methods. 2003;107(1):99–106.
45. Boutsika K, Phillips MS, MacFarlane SA, Brown DJF, Holeva RC, Blok VC. Molecular diagnostics of some trichodorid nematodes and associated tobacco rattle virus. Plant Pathol. 2004;53(1):110–6.
46. Mahillon M, Kellenberger I, Dubuis N, Brodard J, Bunter M, Weibel J, et al. First report of tomato brown rugose fruit virus in tomato in Switzerland. New Disease Rep. 2022;45(1):e12065.
47. Bolger AM, Lohse M, Usadel B. Trimmomatic: a flexible trimmer for illumina sequence data. Bioinformatics. 2014;30(15):2114–20.
48. Prjibelski A, Antipov D, Meleshko D, Lapidus A, Korobeynikov A. Using spades de Novo assembler. Curr Protocols Bioinf. 2020;70(1):e102.
49. Waterhouse AM, Procter JB, Martin DMA, Clamp M, Barton GJ. Jalview version 2–a multiple sequence alignment editor and analysis workbench. Bioinformatics. 2009;25(9):1189–91.
50. Okonechnikov K, Golosova O, Fursov M. UGENE team. Unipro UGENE: a unified bioinformatics toolkit. Bioinformatics. 2012;28(8):1166–7.
51. Edgar RC. MUSCLE: multiple sequence alignment with high accuracy and high throughput. Nucleic Acids Res. 2004;32(5):1792–7.
52. Kalyaanamoorthy S, Minh BQ, Wong TKF, von Haeseler A, Jermiin LS. ModelFinder: fast model selection for accurate phylogenetic estimates. Nat Methods. 2017;14(6):587–9.
53. Nguyen LT, Schmidt HA, von Haeseler A, Minh BQ. IQ-TREE: a fast and effective stochastic algorithm for estimating maximum-likelihood phylogenies. Mol Biol Evol. 2015;32(1):268–74.
54. Hoang DT, Chernomor O, von Haeseler A, Minh BQ, Vinh LS. UFBoot2: improving the ultrafast bootstrap approximation. Mol Biol Evol. 2018;01(2):518–22.
55. Letunic I, Bork P. Interactive tree of life (iTOL) v4: recent updates and new developments. Nucleic Acids Res. 2019;47(W1):W256–9.
56. Gruber AR, Lorenz R, Bernhart SH, Neuböck R, Hofacker IL. The Vienna RNA websuite. Nucleic Acids Res. 2008;36:W70–74.
57. Grigoriev IV, Nikitin R, Haridas S, Kuo A, Ohm R, Otillar R, et al. MycoCosm portal: gearing up for 1000 fungal genomes. Nucleic Acids Res. 2014;42(Database issue):D699–704.
58. Wylie SJ, Tran TT, Nguyen DQ, Koh SH, Chakraborty A, Xu W, et al. A Virome from ornamental flowers in an Australian rural town. Arch Virol. 2019;164(9):2255–63.
59. Shi M, Lin XD, Tian JH, Chen LJ, Chen X, Li CX, et al. Redefining the invertebrate RNA virosphere. Nature. 2016;540(7634):539–43.
60. Velasco L, Arjona-Girona I, Cretazzo E, López-Herrera C. Viromes in xylariaceae fungi infecting avocado in Spain. Virology. 2019;532:11–21.
61. Li W, Sun H, Cao S, Zhang A, Zhang H, Shu Y et al. Extreme diversity of mycoviruses present in single strains of rhizoctonia cerealis, the pathogen of wheat Sharp eyespot. Microbiol Spectr 2023;11(4):e00522–23.
62. Miyauchi S, Kiss E, Kuo A, Drula E, Kohler A, Sánchez-García M, et al. Large-scale genome sequencing of mycorrhizal fungi provides insights into the early evolution of symbiotic traits. Nat Commun. 2020;11(1):5125.
63. Holmes EC. The evolution of endogenous viral elements. Cell Host Microbe. 2011;10(4):368–77.
64. Hernandez C, Carette JE, Brown DJ, Bol JF. Serial passage of tobacco rattle virus under different selection conditions results in deletion of structural and nonstructural genes in RNA 2. J Virol. 1996;70(8):4933–40.
65. Lister RM, Bracker CE. Defectiveness and dependence in three related strains of tobacco rattle virus. Virology. 1969;37(2):262–75.
66. Telengech P, Hyodo K, Ichikawa H, Kuwata R, Kondo H, Suzuki N. Replication of single viruses across the kingdoms, fungi, plantae, and animalia. Proc Natl Acad Sci. 2024;121(25):e2318150121.

Publisher's note